

STATISTICAL RELATIONSHIPS BETWEEN VARIATIONS OF THE GEOMAGNETIC FIELD, AURORAL ELECTROJET, AND GEOMAGNETICALLY INDUCED CURRENTS

A.V. Vorobev

Ufa State Aviation Technical University,
Ufa, Russia, geomagnet@list.ru

V.A. Pilipenko

Schmidt Institute of Physics of the Earth, RAS,
Moscow, Russia, pilipenko_va@mail.ru
Geophysical Center, RAS,
Moscow, Russia, pilipenko_va@mail.ru

Ya.A. Sakharov

Polar Geophysical Institute, RAS, Apatity,
Russia, sakharov@pgia.ru

V.N. Selivanov

Northern Energetics Research Centre KSC RAS, Apatity,
Russia, selivanov@ien.kolasc.net.ru

Abstract. Using observations from the IMAGE magnetic observatories and the station for recording geomagnetically induced currents (GIC) in the electric transmission line in 2015, we examine relationships between geomagnetic field and GIC variations. The GIC intensity is highly correlated ($R > 0.7$) with the field variability $|d\mathbf{B}/dt|$ and closely correlated with variations in the time derivatives of X and Y components. Daily variations in the mean geomagnetic field variability $|d\mathbf{B}/dt|$ and GIC intensity have a wide night maximum, associated with the electrojet, and a wide morning maximum, presumably caused by intense Pc5–Pi3 geomagnetic pulsations. We have constructed a regression linear

model to estimate GIC from the time derivative of the geomagnetic field and AE index. Statistical distributions of the probability density of the AE index, geomagnetic field derivative, and GIC correspond to the log-normal law. The constructed distributions are used to evaluate the probabilities of extreme values of GIC and $|d\mathbf{B}/dt|$.

Keywords: geomagnetic field, geomagnetic variations, geomagnetically induced currents, auroral electrojet.

INTRODUCTION

Research into space weather problems is stimulated, on the one hand, by the fundamental scientific interest in Earth's geophysical layers as an integrated dynamic system; on the other, by the need to ensure stable operation of technological systems. One of the most significant space weather effects is geomagnetically induced currents (GIC) in energy systems, pipelines, and cable systems during magnetic storms and substorms. With technological advances, energy systems (overhead transmission lines (OTL), relay lines, transformer substations) are becoming increasingly vulnerable to space weather disturbances [Sushko, Kosykh, 2013]. Modern energy systems with a highly complex geometry are in fact a giant antenna electromagnetically conjugated with currents of Earth's ionosphere. In grounded systems during magnetic storms, GIC up to 200–300 A were observed [Pirjola et al., 2003], while currents with an intensity of only several amperes are sufficient to put some types of transformers out of the linear mode [Vakhnina, 2012]. Although the most powerful geomagnetic disturbances, which excite intense GIC in energy transmission lines, occur at auroral latitudes, it has recently been found that hazardous GIC intensities can also be observed at middle and low latitudes [Kelly et al., 2017].

Diagnostics and prediction of GIC levels for geomagnetic disturbances of various types, which can be used by transmission system operators to take the necessary steps to reduce the risk of disastrous consequences, are an urgent problem. The solution of this problem is not simply an engineering use of space physics results

to calculate GIC in specific technological systems – it requires understanding the physical nature of some magnetosphere–ionosphere phenomena. The strongest magnetic field disturbances at Earth's surface are driven by an extended auroral electrojet creating magnetic disturbances, oriented in a longitudinal (N-S) direction and posing a risk primarily to technological systems extending in a latitudinal (E-W) direction [Boteler et al., 1998]. A significant contribution to the rapid changes in the magnetic field, essential for GIC, can be made, however, by small-scale ionospheric current structures generating nearly isotropic disturbances of fields and currents [Viljanen, 1997; Belakhovsky et al., 2018]. Nature of these structures and laws of their occurrence remain to be seen.

Geophysical literature has described many individual events in which a relationship is observed between geomagnetic field and GIC variations during such space weather manifestations as interplanetary shocks [Fiori et al., 2014; Pilipenko et al., 2018], explosive substorm commencements [Viljanen et al., 2006], and magnetic storms [Kappenman, 2005]. At the same time, statistical studies of the relationship between geomagnetic field and GIC variations are extremely few in number [Viljanen, Tanskanen, 2011]. Studies of space weather effects on technological systems are hindered by the lack of databases on the malfunction of technological systems available for scientific analysis. This work is largely based on data from Russia's unique system for detecting GIC in OTL on the Kola Peninsula and in Karelia [Sakharov et al., 2007, 2009].

The paper presents the statistical characteristics for 2015, which describe the relationship between geomagnetic disturbances, geomagnetic field variability, geomagnetic indices (*AE*, *PCN*), and GIC. In the case of a closed wire in vacuum, the GIC intensity would be completely determined by the law of electromagnetic induction, i.e. by the time derivative of the geomagnetic field $d\mathbf{B}/dt$. In reality, even in the simplest case, GIC occurs in a spatially distributed system formed by OTL, substations with poorly known characteristics, and underlying layers with frequency-dependent anisotropic geoelectric properties. There cannot, therefore, be a simple characteristic of the geomagnetic field dynamics completely determining the GIC intensity. For practical applications, it is important to assess what GIC can be expected during different geomagnetic disturbances. Knowledge of these empirical relationships is required to construct diagnostic models of GIC, relying on common space weather parameters characterizing the state of the interplanetary medium and magnetosphere.

INITIAL DATA AND THEIR PREPROCESSING

In the system for recording effects of magnetospheric disturbances on OTL on the Kola Peninsula and in Karelia, a measured parameter (1-min time resolution) is a quasi-constant current flowing in the solid-earthed neutral of a transformer, which is connected with GIC in OTL. A detailed description of this system is available on the website [<http://eurisgic.org>], devoted to the study of effects of geomagnetic disturbances on European energy systems. For this study, we have selected the Vykhodnoi station (VKH) (68.83° N, 33.08° E), which records GIC in the main feed of 330 kV.

Since in the vicinity of OTL it is impossible to make magnetometric observations, we have used data from magnetic stations of the IMAGE magnetometer network [www.geo.fmi.fi/image]. We utilized 10 s data from magnetic observatories nearest to the GIC station: IVA (68.56° N, 27.29° E, a distance away of 236 km), KEV (69.76° N, 27.01° E, a distance away of 260 km), and SOD (67.37° N, 26.63° E, a distance away of 313 km). The IVA station is located at the same geomagnetic latitude as VKH. All time series used in this paper have been decimated to a sampling increment of 1 min. To eliminate the influence of high-frequency components during the decimation, we applied a digital flat-top band-pass filter [Dvorkovich, Dvorkovich, 2014].

As global space weather characteristics at auroral and polar latitudes we used the 1-min indices *AE* [<http://wdc.kugi.kyoto-u.ac.jp/aedir>] and *PCN* [<http://www.geophys.aari.ru>]. The *AE* index represents the planetary geomagnetic field disturbance at auroral latitudes, caused by the auroral electrojet. The *PCN* index, calculated from magnetic observations in the north polar cap, describes the energy transferred from the solar wind to the magnetosphere [Stauning, 2018].

At the initial stage, we unified and analyzed completeness and interrelation of time series of observations from magnetic and GIC stations, as well as *AE* and *PCN* indices. The analysis of completeness of the time series

showed that in 2015 VKH omitted 1.625 % of values; IVA, 4.9 %; SOD, 0.13 %; KEV, 0.01 %; 8.5 % of the omitted values are in *AE*; and 4.6 %, in *PCN*. For the cross-sectional analysis, we can use ~93.3 % of the total amount of data (490 385 values).

For continuous time series, we calculated disturbances of the horizontal geomagnetic field component $\Delta\mathbf{B}=\{\Delta X, \Delta Y\}$ (X -N-S and Y -E-W field components) and the first time derivatives $d\mathbf{B}/dt=\{dX/dt, dY/dt\}$, nT/min. With horizontal uniformity of geoelectric properties of underlying layer, the orientation of the vector $d\mathbf{B}/dt$ corresponds to the orientation of the excited telluric field \mathbf{E} . The $\Delta\mathbf{B}$ values were calculated relative to \mathbf{B}_0 (the daily mean of $\mathbf{B}(t)$ at a given magnetic station). At auroral latitudes, a magnetic disturbance can be caused by both the westward and eastward electrojets, which shows up in a decrease or an increase in the X component respectively ($\Delta X < 0$ or $\Delta X > 0$). To avoid the difficulties in changing the sign of magnetic disturbance, hereinafter we use the absolute values of $|\Delta X|$, $|\Delta Y|$. As a unified characteristic of the field variability in time we use the absolute values of both the derivatives of horizontal components $|dX/dt|$ and $|dY/dt|$ and the total derivative $|d\mathbf{B}/dt| = \sqrt{(dX/dt)^2 + (dY/dt)^2}$.

DIURNAL VARIATION OF GEOMAGNETIC DISTURBANCES AND GIC

We have constructed histograms of averages of different characteristics of geomagnetic disturbances and GIC for 2015 for 1-hr local time (LT) intervals. The diurnal variation of the global *AE* index has no pronounced maxima and minima (not shown). The calculation of the diurnal variation of magnetic disturbance $|\Delta X|$ at IVA (Figure 1, *a*) has shown the presence of midnight (LT~24) and afternoon (LT~15) maxima. These maxima are caused by the intensification of the westward and eastward electrojets over the station during substorm activations.

The diurnal variation of the mean geomagnetic field variability $|d\mathbf{B}/dt|$ at IVA (Figure 1, *b*) has a somewhat different character, with wide night (LT~21–01) and morning (LT~5–6) maxima. The night maximum is most likely to be associated with the electrojet. The increased field variability in the morning is presumably caused by intense Pc5-Pi3 geomagnetic pulsations observed most often in early morning hours [Kleimenova, Kozyreva, 2004; Pahud et al., 2009]. The appearance of large values of the time derivative of the geomagnetic field during the occurrence of Pi3 pulsations has been observed by Yagova et al. [2018]. The diurnal variation of the average GIC intensity at VKH repeats that of the geomagnetic field variability $|d\mathbf{B}/dt|$ (Figure. 1, *c*).

The calculation of the diurnal variation of $d\mathbf{B}/dt$ for a long-term period at high-latitude IMAGE stations, made by Viljanen and Tanskanen [2011], has also shown the presence of the morning and midnight maxima whose relative values varied with season. The reconstruction of the

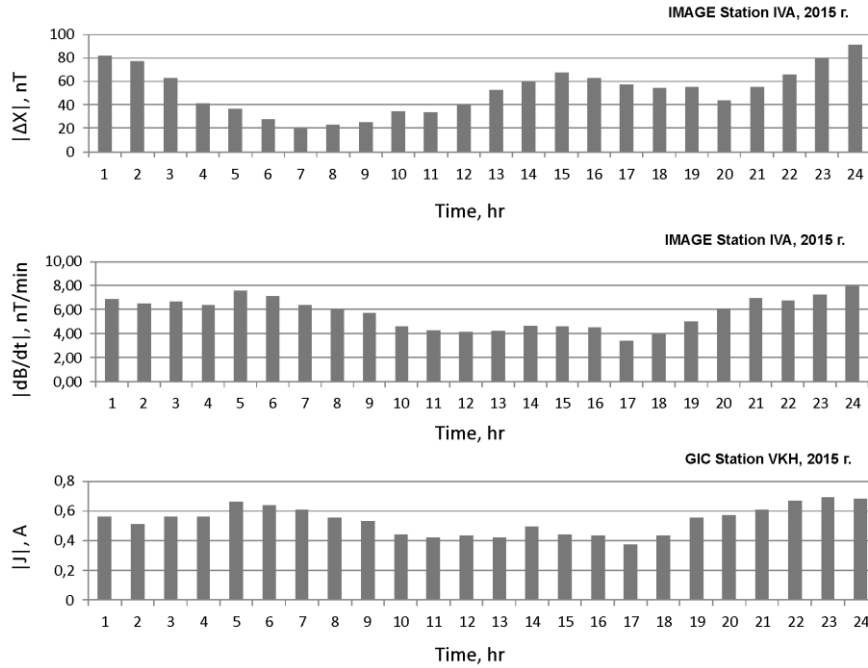


Figure 1. Diurnal variations of average magnetic disturbance $|\Delta X|$ (a), geomagnetic field variability $|dB/dt|$ (b), and GIC intensity $|J|$ (at IVA for 2015) (c)

auroral electrojet along the meridian of $\sim 22^\circ$ E according to IMAGE data gave the following regularities of the diurnal variation: the eastward electrojet prevails in the afternoon hours (13–21 MLT), the westward electrojet prevails in the remaining hours, peaking at $\sim 01:30$ MLT. Our results confirm that the morning maximum in the diurnal variation of $|dB/dt|$ has no correspondence in the distribution of the intensity of electrojet-driven geomagnetic disturbances $|\otimes X|$; and in the maximum eastward electrojet there is no increase in the level of variations in $|dB/dt|$.

CORRELATION RELATIONSHIPS BETWEEN GIC, FIELD VARIABILITY, AND GEOMAGNETIC INDICES

Knowledge of statistical relationships is required as a first step for developing diagnostic models of GIC with the use of general space weather characteristics [Weigel et al., 2003]. Let us figure out how sufficient the geomagnetic indices characterizing substorm activity (*AE*, *PCN*, etc.) are to predict the GIC intensity. To do this, we calculate the correlation relationships between the absolute GIC value $|J|$, recorded by VKH, and the main geomagnetic indices for 2015. The cross-correlation function $R(\tau)$ of the studied time series is maximum for $\tau = 0$. It should be kept in mind that correlation coefficients for a particular time interval may differ from annual average values and vary from 0.2 to 0.95.

The maximum correlation is observed between $|J|$ and global indices *AE* ($R=0.56$) and *AL* ($R=0.55$). The correlation with *AU* is lower: $R=0.44$. Thus, when modeling and predicting GIC variations, our main concern is with the behavior of the *AE* index. While it is believed that the *PCN* index well characterizes substorm activity, the GIC corre-

lation with *AE* is higher than with *PCN* ($R=0.44$).

Let us see how sufficient the local geomagnetic field disturbance and variability are to predict the GIC intensity. Table 1 presents the result of calculation of the Pearson correlation coefficient R between the absolute GIC value $|J|$, recorded by VKH, geomagnetic disturbances $|\Delta X|$, $|\Delta Y|$, and the rate of change in the field components $|dX/dt|$, $|dY/dt|$ at IVA, KEV, and SOD for 2015.

The correlation of $|J|$ with the rate of change in the horizontal magnetic field components $|dX/dt|$ and $|dY/dt|$ is higher than that with the magnitude of the field disturbance $|\Delta X|$, $|\Delta Y|$ on average by 31.5%. In other words, the correlation of GIC with the time derivative of the field is closer than with the field disturbance.

The correlation coefficients of $|J|$ with variations in the X and Y derivatives are similar. This result confirms that the field derivative dB/dt fluctuates not only in magnitude but also in direction, which may be associated with the presence of rapidly varying local vortex structures superimposed on the magnetic field of the auroral electrojet [Viljanen, 1997].

The contribution of the rapid geomagnetic field variations may be different for periods of magnetic storms and undisturbed periods. To test this assumption, we calculated the correlation coefficients between GIC and geomagnetic field variability at different magnetic stations for the March 17–18, 2015 magnetic storm (St. Patrick’s Day magnetic storm) from 06 UT on March 17, 2015 to 06 UT on March 18, 2015 (Table 1, bottom row). During the storm, the correlation between GIC and geomagnetic field variability was almost the same as on average during the year (Table 1, top row). In this case, the correlation of $|J|$ with $|dY/dt|$ is even somewhat higher than that with $|dX/dt|$. Thus, the contribution of

the Y variability to the $|J|$ intensity is comparable with the contribution of the X variability for both disturbed and undisturbed periods.

The question arises how well the geomagnetic indices AE and PCN describing substorm activity characterize the geomagnetic field variability, i.e. $d\mathbf{B}/dt$. To answer this question, we calculated the correlation between these indices and $|dX/dt|$, $|dY/dt|$ from the data for 2015 (Table 2, top row).

The AE index correlates well with $|\Delta X|$, which is natural because this index is calculated from data on magnetic disturbances at auroral stations. The field variability also depends on substorm activity, characterized by the AE index. The correlation coefficient between the field variability and $AER \sim 0.6$ corresponds, however, to the determi-

nation coefficient $D=R^2 \sim 0.36$, i.e. the field variability $|d\mathbf{B}/dt|$ is determined by the electrojet intensity (AE) only by $\sim 40\%$.

To find out how much the correlation between AE and PCN and the field variability changes during magnetic storms, we calculated the correlation coefficients between them for the March 17–18, 2015 magnetic storm (Table 2, the second and third rows). For the storm period, we observed a high correlation between AE and $|dX/dt|$: $R \sim 0.8$, than the average for the year: $R \sim 0.6$. The analysis of the correlation between the time series of PCN and $|dX/dt|$ shows a similar pattern (Table 2, bottom row).

Table 1

Correlation coefficients R between $ J $ and geomagnetic variations in the magnetic stations nearest to VKH												
	IVA				SOD				KEV			
	$ \Delta X $	$ dX/dt $	$ \Delta Y $	$ dY/dt $	$ \Delta X $	$ dX/dt $	$ \Delta Y $	$ dY/dt $	$ \Delta X $	$ dX/dt $	$ \Delta Y $	$ dY/dt $
2015	0.493	0.696	0.442	0.672	0.488	0.679	0.430	0.627	0.478	0.679	0.427	0.677
Storm		0.623		0.713		0.617		0.699		0.547		0.644

Table 2

Correlation coefficients R of AE and PCN
with variations and variability of the X and Y components

	IVA				SOD				KEV			
	$ \Delta X $	$ dX/dt $	$ \Delta Y $	$ dY/dt $	$ \Delta X $	$ dX/dt $	$ \Delta Y $	$ dY/dt $	$ \Delta X $	$ dX/dt $	$ \Delta Y $	$ dY/dt $
2015	0.643	0.585	0.504	0.582	0.643	0.614	0.493	0.576	0.631	0.549	0.513	0.572
AE storm		0.846		0.585		0.768		0.751		0.803		0.264
PCN storm		0.911		0.641		0.872		0.821		0.799		0.309

REGRESSION MODEL OF GIC

For applied assessments it is important to know what GIC can be expected at the current state of the electrojet, characterized by the AE index, and the geomagnetic field variability level. To answer this question, we synthesized the linear regression model, which generally takes the form

$$|J| = w_0 + \sum_{i=1}^N (w_i C_i) \pm \Delta, \quad (1)$$

where C_i are driving parameters ($i = 1, N$); w are weight coefficients of the model; \oplus is the average modeling error. Model (1) allows us to statistically estimate $|J|$ from N control parameters C_i . If the model is constructed using all recorded values, it will be determined by minor GIC disturbances which are not very interesting. To construct a regression model, we should therefore select values greater than a certain threshold. This causes the w coefficients to increase.

Linear regression models were built for the AE index and magnetic field variability $|d\mathbf{B}/dt|$ at IVA for two months (from March 1 to April 30, 2015) – the longest interval without gaps in all analyzed parameters.

$$|J| = w_0 + w_1 |d\mathbf{B}/dt| \pm \Delta_1; \quad (2)$$

$$|J| = w_0 + w_2 |AE| \pm \Delta_2.$$

The weight coefficients w_1 , w_2 in expressions (2)

were calculated using the gradient descent method.

The calculation for 2015 by the reduced model (with the exception of $|d\mathbf{B}/dt| < 1$ nT/min from the sample) for IVA yields the following coefficients: $w_0 = 0$, $w_1 = 0.074$ A·min/nT and $w_2 = 0.0022$ A/nT. Figure 2 compares simulated GIC values with the observed ones for the period of the March 17, 2015 complex magnetic storm with a series of substorm activations. The comparison of predictions of models (2) with the measured values shows that the model based on the AE index predicts well the moments of the occurrence of GIC, but not their intensity. The model based on $|d\mathbf{B}/dt|$ predicts well the moments of GIC amplification and their intensity, but underestimates their extreme values. In the time interval of interest, models (2) give average errors $\Delta_1 = \pm 0.91$ A and $\Delta_2 = \pm 1.78$ A. Thus, it is most appropriate to use the regression model with $|d\mathbf{B}/dt|$ to assess GIC variations. In principle, we can estimate the possible level of GIC variations in OTL from current AE values, but it is suitable for a more narrow range of values; in this case, the standard error would increase by $\sim 50\%$.

In general, the statistical model works well (small Δ_1) for intermediate $|d\mathbf{B}/dt|$, whose probability is not less than $\sim 1\%$ (which statistically represents $|d\mathbf{B}/dt| < 40$ nT/min and $|J| < 3$ A) and for the intermediate AE index whose probability is not less than $\sim 24\%$ (which statistically represents $AE < 300$ nT and $|J| < 0.7$ A). For $|J| > 20$ A, the regression model based on field variability data has the form of (2) for $\Delta_1 = \pm 2.3$ A, $w_0 = 11.677$ A, and $w_1 = 0.11$ A·min/nT.

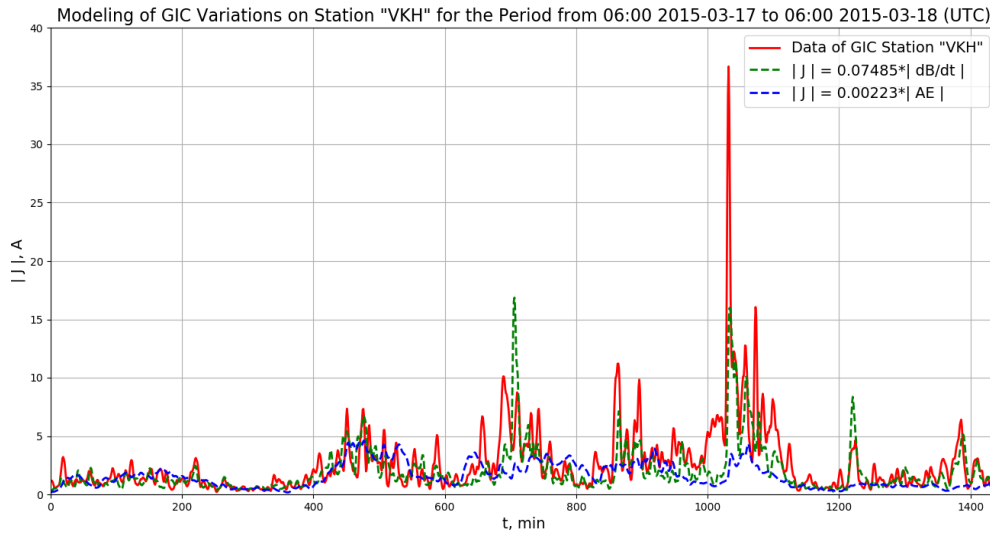


Figure 2. Result of GIC modeling for the March 17, 2015 storm from 00:00 to 24:00 UT

STATISTICAL DISTRIBUTIONS OF GIC AND GEOMAGNETIC FIELD VARIATIONS

The form of the probability function $F(x)$ of the disturbance amplitude x is determined by physical mechanisms of the process under study. So, under random independent actions, a normal (Gaussian) distribution is formed; in a closed system the energy of its components is distributed according to the exponential Boltzmann-Laplace law; the self-similar distribution (Pareto) according to the power law is often attributed to the self-organized criticality; the random multiplicative selection from several parameters leads to a log-normal distribution, etc.

Of great importance is the presence of heavy tails of distribution [Pisarenko, Rodkin, 2007]. With these power distributions, the variance of the magnitude considered is mainly determined by rare intense deviations, not by frequent small deviations. If we do not know to the full the nature of distribution, and use only averages, we can come to false conclusions about properties of the system.

The most close among the distributions commonly found in geophysical research [Chisham, Freeman, 2010] for the values considered proved to be the log-normal distribution (σ is the shape parameter)

$$F(x) = \frac{1}{\sigma x \sqrt{2\pi}} \exp\left(-\frac{1}{2} \left(\frac{\ln(x)}{\sigma}\right)^2\right) \quad (3)$$

and the generalized power Pareto distribution (shape parameter $c > 0$)

$$F(x) = (1 + cx)^{-1-\frac{1}{c}}. \quad (4)$$

The normalized histogram of $F(x)$ gives the probability density distribution, i.e. each value is the probability of observation of a given x at a given interval Δx during the period analyzed. Figure 3 shows normalized histograms of the AE probability density for 2015. The analysis of the normalized histograms has revealed that the AE probability

density distribution most closely corresponds to the log-normal distribution (see Figure 3, Table 3).

Figure 4 presents the normalized histograms of the X -component disturbance at SOD for 2015. According to Table 3, the $|\Delta X|$ probability density distribution most closely corresponds to generalized Pareto distribution (3).

Histograms of $|dB/dt|$ are given in Figure 5; and of $|J|$, in Figure 6. The $|dB/dt|$ and $|J|$ probability density distribution is best approximated by the log-normal distribution.

The results shown in Figures 4 and 5 for SOD are similar for IVA and KEV and are not given here.

The resulting non-Gaussian distributions allow us to correctly determine the median, expectation, and probability of observation of the parameters analyzed in the given range, to estimate whether the recorded values belong to abnormal ones. The knowledge of the statistical distribution of fluctuation probability enables us to estimate the probability of an extreme event, which even cannot be observed during the observation period (assuming that it obeys the same laws) [Pulkkinen et al., 2012]. From the probability curve (Figures 3–6) we can statistically estimate which maximum disturbance of AE , dB/dt , and J is possible for the given period of observation. The statistics show that in 2015 $|AE| > 1000$ nT were observed during $\sim 1\%$ of time; $|J| > 10$ A, during $\sim 0.03\%$ of time; and $|dB/dt| > 60$ nT/min, during $\sim 0.2\%$ of time.

With a probability of $\sim 0.01\%$ (about 50 times a year) there may be disturbances with $|AE| > 2000$ nT, regional GIC and magnetic field disturbances with $|J| > 13$ A, $|dB/dt| > 113$ nT/min, and $|\Delta X| > 880$ nT. Significant GIC variations ($|J| > 1$ A) occur with a probability of $\sim 9.7\%$.

Evaluating and analyzing statistical characteristics of the time series under study, we can talk about the similarity in their statistics, and, hence, about the similarity in their physical mechanisms. To test the hypothesis that the analyzed sample belongs to the known distribution law,

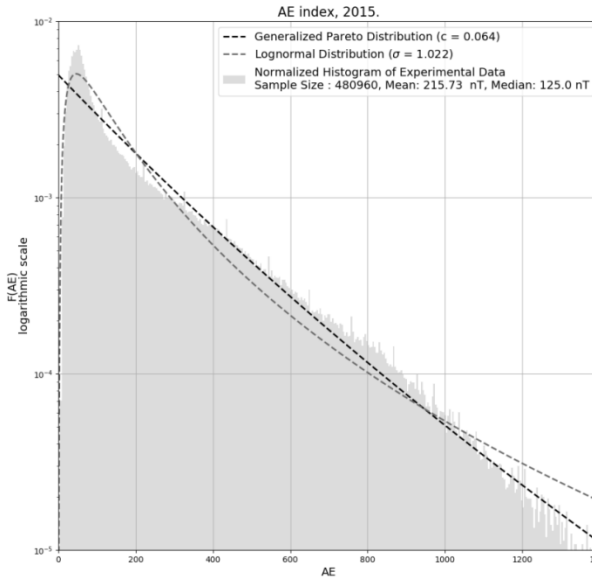


Figure 3. Distributions of AE probability density for 2015

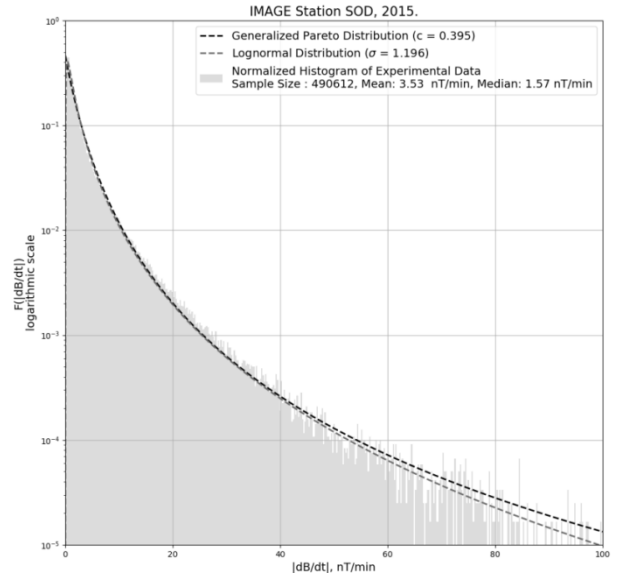


Figure 5. Distributions of $|dB/dt|$ probability density for SOD for 2015

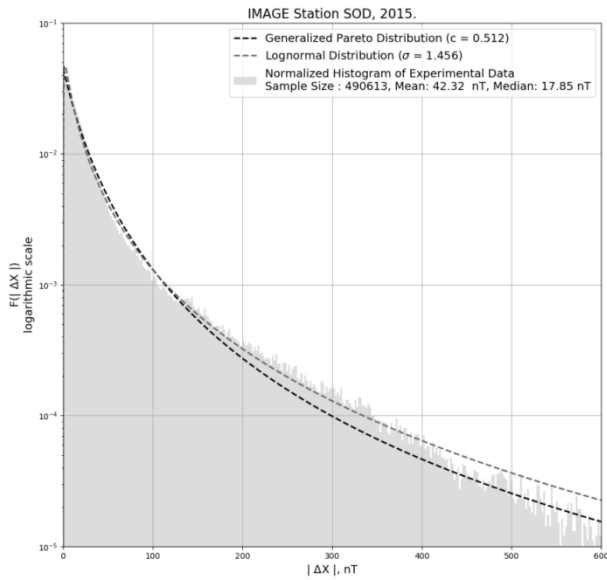


Figure 4. Distributions of $|\Delta X|$ probability density for SOD for 2015

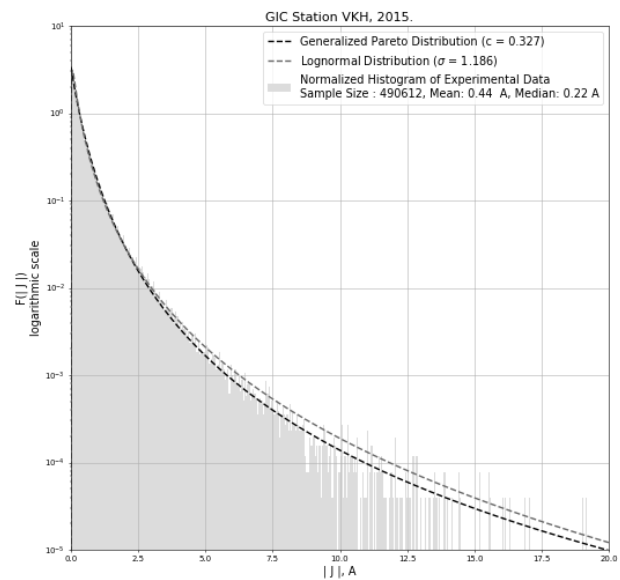


Figure 6. Distribution of GIC probability density for VKH for 2015

we used the Kolmogorov criterion characterizing the absolute maximum difference between experimental curves and the inferred known distribution: distribution with a minimum value of this criterion best describes the statistics of the experimental sample (Table 3).

Thus, according to Table 3, we can conclude that the $|\Delta X|$ distribution statistics are fairly well described by the generalized Pareto distribution, whereas the AE index, field and GIC variability better corresponds the log-normal distribution (according to [Bolshev, Smirnov, 1983] the proposed hypotheses can be rejected with a significance level of no more than 0.01 %). Note that numerous studies on statistical properties of the AE index (e.g., [Consolini, de Michelis, 1998]) indicate that quiet periods; and another, to substorm periods.

The fact that both the $F(|J|)$ and $F(|dB/dt|)$ probability distributions have the form similar to the log-normal the AE distribution is best simulated by the sum of two log-normal distributions, one of which corresponds to

Table 3
Kolmogorov criterion for distributions of geomagnetic variations and GIC

Time series / Distribution	AE	$ X $	$ dB/dt $	$ J $
log-normal	0.0558	0.0342	0.0249	0.0185
generalized Pareto	0.0795	0.0206	0.0647	0.0649

one may indicate that these distributions result from the multiplicative stochastic effect. It is interesting to note that the near-Earth plasma turbulence, as derived from many observations, is often described by the log-normal distribution too [Kozak et al., 2012]. Thus, such a coincidence may indicate that the near-Earth plasma turbulence is largely responsible for the geomagnetic field variability, and hence for the occurrence of GIC.

It seems likely that, with planetary indices (of *AE* type), we cannot identify the conditions under which the extreme currents occur at the selected substation. These indices can be useful for estimating the total GIC in all nodes of regional OTL. GIC can more precisely characterize regional geomagnetic indices such as the proposed *IE* index (IMAGE Electrojet Indicator, [<http://space.fmi.fi/image/www>]). The intensity of the local GIC is determined not only by the local value of $d\mathbf{B}/dt$ and geoelectric conditions but also by the spatial relationships between OTL size and scale of fast geomagnetic disturbances [Yagova et al., 2016].

CONCLUSION

According to the data for 2015, the correlation between GIC and variability of geomagnetic field components $|dX/dt|$ and $|dY/dt|$ can be characterized as high ($R > 0.7$); and between GIC and magnetic disturbances $|\Delta X|$, $|\Delta Y|$ and the *AE* index, as significant ($0.5 < R < 0.7$) both on average for the year and during a magnetic storm. In this case, the correlation coefficients between $|J|$ and variations in the *X* and *Y* derivatives proved to be similar, thus confirming the previously mentioned quasi-isotropism of rapid variations in the geomagnetic field derivative $d\mathbf{B}/dt$ [Viljanen, 1997; Belakhovsky et al., 2018].

Daily variations in the mean geomagnetic field variability $|d\mathbf{B}/dt|$ and GIC intensity have a wide night maximum, associated with the electrojet, and a wide morning maximum, presumably caused by intense Pc5–Pi3 geomagnetic pulsations.

The regression linear diagnostic model with $|d\mathbf{B}/dt|$ as an input parameter predicts that GIC will be moderate with an average error of ± 0.91 A; and the model based on the *AE* index, with an error of $\sim 50\%$ larger. Large values of GIC ($20 < |J| < 45$ A) can be predicted from the parameter $|d\mathbf{B}/dt|$ with a mean accuracy of ± 2.3 A.

The probability density of $|d\mathbf{B}/dt|$, $|J|$, and *AE* most closely corresponds to the log-normal distribution; and the $|\Delta X|$ probability density, to the generalized Pareto distribution.

This work was supported by the Russian Science Foundation (grant No. 16-17-00121). We thank the research teams engaged in the operation of the magnetometer network IMAGE [<http://space.fmi.fi/image>] and calculating the *AE* and *PCN* indices. We are grateful to reviewers for their careful study of the manuscript and valuable comments.

REFERENCES

Belakhovsky V.B., Sakharov Y.A., Pilipenko V.A., Selivanov V.N. Characteristics of the variability of a geomagnetic field for studying the impact of the magnetic storms and substorms on electrical energy systems. *Izvestiya. Physics of the Solid Earth*. 2018, vol. 54, no. 1, pp. 52–65. DOI: [10.1134/S1069351318010032](https://doi.org/10.1134/S1069351318010032).

Boteler D.H., Pirjola R.J., Nevanlinna H. The effects of geomagnetic disturbances on electrical systems at the Earth's surface. *Adv. Space Res.* 1998, vol. 22, iss. 1, pp. 17–27. DOI: [10.1016/S0273-1177\(97\)01096-X](https://doi.org/10.1016/S0273-1177(97)01096-X).

Bolshev L.N., Smirnov N.V. *Tablitsy matematicheskoi statistiki* [Tables of Mathematical Statistics]. Moscow, Nauka

Publ., 1983, 416 p. (In Russian).

Chisham G., Freeman M.P. On the non-Gaussian nature of ionospheric vorticity. *Geophys. Res. Lett.* 2010, vol. 37, iss. 12, L12103. DOI: [10.1029/2010GL043714](https://doi.org/10.1029/2010GL043714).

Consolini G., de Michelis P. Non-Gaussian distribution function of *AE*-index fluctuations: evidence for time intermittency. *Geophys. Res. Lett.* 1998, vol. 25, iss. 21, pp. 4087–4090. DOI: [10.1029/1998GL900073](https://doi.org/10.1029/1998GL900073).

Dvorkovich V.P., Dvorkovich A.V. *Okonnye funktsii dlya garmonicheskogo analiza signalov* [Window Functions for Harmonic Analysis of Signals]. Moscow, Technosfera Publ., 2014, 112 p. (In Russian).

Fiori R.A.D., Boteler D.H., Gillies D.M. Assessment of GIC risk due to geomagnetic sudden commencements and identification of the current systems responsible. *Space Weather*. 2014, vol. 12, iss. 1, pp. 76–91, DOI: [10.1002/2013SW000967](https://doi.org/10.1002/2013SW000967).

Kappenman J.G. An overview of the impulsive geomagnetic field disturbances and power grid impacts associated with the violent Sun–Earth connection events of 29–31 October 2003 and a comparative evaluation with other contemporary storms. *Space Weather*. 2005, vol. 3, iss. 1, S08C01. DOI: [10.1029/2004SW000128](https://doi.org/10.1029/2004SW000128).

Kelly G.S., Viljanen A., Beggan C., Thomson A.W.P. Understanding GIC in the UK and French high-voltage transmission systems during severe magnetic storms. *Space Weather*. 2017, vol. 15, iss. 1, pp. 99–114. DOI: [10.1002/2016SW001469](https://doi.org/10.1002/2016SW001469).

Kleimenova N.G., Kozyreva O.V. Spatio-temporal dynamics of geomagnetic pulsations Pi3 and Pc5 during extreme magnetic storms in October 2003. *Geomagnetism and Aeronomy*. 2005, vol. 45, no. 1, pp. 71–79.

Kozak L.V., Savin S.P., Budaev V.P., Pilipenko V.A., Lezhen L.A. Character of turbulence in the boundary regions of the Earth's magnetosphere. *Geomagnetism and Aeronomy*. 2012, vol. 52, no. 4, pp. 445–455. DOI: [10.1134/S0016793212040093](https://doi.org/10.1134/S0016793212040093).

Pahud D.M., Rae I.J., Mann I.R., Murphy K.R., Amalraj V. Ground-based Pc5 ULF wave power: solar wind speed and MLT dependence. *J. Atmos. Solar-Terr. Phys.* 2009, vol. 71, iss. 10–11, pp. 1082–1092. DOI: [10.1016/j.jastp.2008.12.004](https://doi.org/10.1016/j.jastp.2008.12.004).

Pilipenko V.A., Bravo M., Romanova N.V., Kozyreva O.V., Samsonov S.N., Sakharov Y.A. Geomagnetic and ionospheric responses to the interplanetary shock wave of March 17, 2015. *Izvestiya. Physics of the Solid Earth*. 2018, vol. 54, no. 5, pp. 721–740. DOI: [10.1134/S1069351318050129](https://doi.org/10.1134/S1069351318050129).

Pirjola R., Pulkkinen A., Viljanen A. Studies of space weather effects on the Finnish natural gas pipeline and on the Finnish high-voltage power system. *Adv. Space Res.* 2003, vol. 31, iss. 4, pp. 795–805. DOI: [10.1016/S0273-1177\(02\)00781-0](https://doi.org/10.1016/S0273-1177(02)00781-0).

Pisarenko V.F., Rodkin M.V. *Raspredeleyeniya s tyazhelyimi khvostami: prilozheniya k analizu katastrof* [Distributions with Heavy Tails: Applications to the Analysis of Disasters]. Moscow, GEOS Publ., 2007, 242 p. (In Russian).

Pulkkinen A., Bernabeu E., Eichner J., Beggan C., Thomson A.W.P. Generation of 100-year geomagnetically induced current scenarios. *Space Weather*. 2012, vol. 10, iss. 4, S04003. DOI: [10.1029/2011SW000750](https://doi.org/10.1029/2011SW000750).

Sakharov Ya.A., Danilin A.N., Ostafiychuk R.M. Registration of GIC in power systems of the Kola Peninsula. *Proc. of 7th Intern. Symp. on Electromagnetic Compatibility and Electromagnetic Ecology*. St. Petersburg, June 26–29, 2007, pp. 291–293.

Sakharov Ya.A., Danilin A.N., Ostafiychuk R.M., Katalov Yu.V., Kudryashova N.V. Geomagnetically induced currents in the power systems of the Kola peninsula at solar minimum. *Proc. of 8th Intern. Symp. on Electromagnetic Compatibility and Electromagnetic Ecology*. St. Petersburg, 2009, pp. 237–238.

Stauning P. Multi-station basis for Polar Cap (PC) indices:

ensuring credibility and operational reliability. *J. Space Weather Space Climate*. 2018, vol. 8, A07, 14 p. DOI: [10.1051/swsc/2017036](https://doi.org/10.1051/swsc/2017036).

Sushko V.A., Kosykh D.A. Geomagnetic storms. The Threat to Russia's National Security. *Novosti elektrotehniki* [News of Electrical Engineering]. 2013, no. 4 (82), pp. 25–28. (In Russian).

Viljanen A. The relation between geomagnetic variations and their time derivatives and implications for estimation of induction risks. *Geophys. Res. Lett.* 1997, vol. 24, pp. 631–634. DOI: [10.1029/97GL00538](https://doi.org/10.1029/97GL00538).

Viljanen A., Tanskanen E. Climatology of rapid geomagnetic variations at high latitudes over two solar cycles. *Ann. Geophys.* 2011, vol. 29, pp. 1783–1792. DOI: [10.5194/angeo-29-1783-2011](https://doi.org/10.5194/angeo-29-1783-2011).

Viljanen A., Tanskanen E.I., Pulkkinen A. Relation between substorm characteristics and rapid temporal variations of the ground magnetic field. *Ann. Geophys.* 2006, vol. 24, pp. 725–733. DOI: [10.5194/angeo-24-725-2006](https://doi.org/10.5194/angeo-24-725-2006).

Vakhnina V.V. *Modelirovanie rezhimov raboty silovykh transformatorov sistem elektrosnabzheniya pri geomagnitnykh buryakh* [Modeling of Operation Modes of Power Transformers of Power Supply Systems in Geomagnetic Storms]. Togliatti, Togliatti State University, 2012. 103 p. (In Russian).

Weigel R.S., Klimas A.J., Vassiliadis D. Solar wind coupling to and predictability of ground magnetic fields and their time derivatives. *J. Geophys. Res.* 2003, vol. 108, no. A7, 1298. DOI: [10.1029/2002JA009627](https://doi.org/10.1029/2002JA009627).

Yagova N.V., Lamondodog A.D., Gusev Yu.P., Pilipenko V.A., Fedorov E.N. Frequencies of occurrence of extreme values of time-derivative geomagnetic fields, potentially dangerous for industrial electric networks, according to data of long-term observations on the IMAGE network. *Proc. of the All-Russian Conference "Heliogeophysical Research in the Arctic"*. Apatity, September 19–23, 2016, pp. 81–84. (In Russian).

Yagova N.V., Pilipenko V.A., Fedorov E.N., Lhamdotong A.D., Gusev Yu.P. Geomagnetically induced currents and space weather: Pi3 pulsations and extreme values of the time derivatives of the horizontal components of the geomagnetic field. *Izvestiya. Physics of the Solid Earth*. 2018, vol. 54, no. 5, pp. 749–763. DOI: [10.1134/S1069351318050130](https://doi.org/10.1134/S1069351318050130).

URL: <http://eurisgic.org> (accessed September 9, 2018).

URL: www.geo.fmi.fi/image (accessed September 9, 2018).

URL: <http://wdc.kugi.kyoto-u.ac.jp/aedir> (accessed September 9, 2018).

URL: <http://www.geophys.aari.ru> (accessed September 9, 2018).

URL: <http://space.fmi.fi/image/www> (accessed September 9, 2018).

URL: <http://space.fmi.fi/image> (accessed September 9, 2018).

How to cite this article

Vorobev A.V., Pilipenko V.A., Sakharov Ya.A., Selivanov V.N. Statistical relationships between variations of the geomagnetic field, auroral electrojet, and geomagnetically induced currents. *Solar-Terrestrial Physics*. 2019. Vol. 5. Iss. 1. P. 35–42. DOI: [10.12737/stp-51201905](https://doi.org/10.12737/stp-51201905).